Exploration of novel metabolic features reflecting statin sensitivity in lung cancer cells

Jiro Tashiro[1], Tomoko Warita[2]*, Akihiro Sugiura[1], Kana Mizoguchi[3], Takuro Ishikawa[1], and Katsuhiko Warita[1]*

[1] Department of Veterinary Anatomy, School of Veterinary Medicine, Tottori University, 4-101 Koyama Minami, Tottori 680-8553, Japan

[2] Department of Biomedical Sciences, School of Biological and Environmental Sciences, Kwansei Gakuin University, 1 Gakuen Uegahara, Sanda, Hyogo 669-1330, Japan

[3] Graduate School of Science and Technology, Kwansei Gakuin University, 1 Gakuen Uegahara, Sanda, Hyogo 669-1330, Japan

* Corresponding author:
Katsuhiko Warita
waritak@tottori-u.ac.jp
ORCID: 0000-0003-2545-6349
Tomoko Warita
waritat@kwansei.ac.jp
ORCID: 0000-0003-4402-375X

Abstract

Statins are cholesterol-lowering drugs often used for the treatment of dyslipidemia. Statins also exert anticancer effects by inhibiting hydroxymethylglutaryl-CoA reductase (HMGCR), a rate-limiting enzyme in cholesterol synthesis. We previously reported that the susceptibility to statin treatment differs among cancer cells and that functional E-cadherin expression on the plasma membrane could be a biomarker of statin sensitivity in cancer cells. However, the detailed qualitative and molecular differences between statin-sensitive and statin-resistant cancer cells remain unclear. Here, we explored novel parameters related to statin sensitivity by comparing gene expression profiles and metabolite contents between statin-sensitive and statin-resistant lung cancer cell lines. We found that the expression of most cholesterol synthesis genes was lower in the statin-sensitive cancer cell line, HOP-92, than in the statin-resistant cancer cell line, NCI-H322M. Moreover, HOP-92 cells originally exhibited lower levels of CoA and HMG-CoA. Additionally, atorvastatin decreased the expression of *PANK2*, a rate-limiting enzyme in CoA synthesis. Atorvastatin also reduced the mRNA levels of the cholesterol esterification enzyme *SOAT1*, which was consistent with a decrease in the ratio of cholesterol ester to total cholesterol in HOP-92 cells. Our data suggest that the mevalonate pathway flow and CoA content may be limited in statin-sensitive cancer cells. We also suggest that CoA synthesis and cholesterol storage fluctuate with atorvastatin treatment in statin-sensitive cancer cells.

Keywords

Cancer, Statin-sensitivity, CoA, Cholesterol, PANK2, SOAT1

Introduction

Statins, therapeutic agents for hypercholesterolemia, exert cholesterol lowering effect by competitively inhibiting hydroxymethylglutaryl-CoA (HMG-CoA) reductase (HMGCR), the rate limiting enzyme in the mevalonate pathway.[1,2] Statins can also induce cell death and inhibit cell growth in many cancer cell types in part due to depletion of geranylgeranyl pyrophosphate (GGPP), a non-sterol intermediate in the mevalonate pathway.[3–7] These observations suggest the potential of statins as anti-cancer agents. However, statins are sometimes ineffective against specific cancer cell types. Although we have previously identified functional E-cadherin as a marker of statin-resistant cancer cells,[8,9] the detailed mechanisms and cellular features related to statin sensitivity have not been completely revealed.

The cholesterol biosynthesis process is regulated through transcriptional and post-transcriptional mechanisms.[10] Inhibition of HMGCR activity with statins can cause feedback response that increases HMGCR expression by activating sterol regulatory element binding protein 2 (SREBP2), a transcription factor of the mevalonate pathway enzymes.[10–13] To date, it has been reported that basal expression of cholesterol biosynthesis genes, including HMGCR, and statin-induced feedback response are correlated with statin sensitivity in cancer cells.[12–15] Moreover, many researchers demonstrated that HMGCR downregulation and SREBP2 inhibition could enhance statins' anti-cancer effects regardless of the origin of the cancer.[6,11–13,16–18]

Thus, studies on statin-resistant cancer have mainly focused on the mevalonate pathway genes. For a more appropriate understanding of statin sensitivity in cancer cells, further analysis focusing on factors other than HMGCR expression is necessary.

Therefore, in addition to cholesterol synthesis enzymes, we focused on CoA and cholesterol metabolism as the initial and subsequent processes in the mevalonate pathway. CoA plays a pivotal role in a number of biochemical processes such as carbohydrate, amino acids, and lipid metabolism.[19] Phosphorylation of pantothenate (Vitamin B_5), the rate limiting step in CoA synthesis, is catalyzed by pantothenate kinase coded by *PANK* genes.[19] Moreover, in the mevalonate pathway, CoA is an essential molecule as a component of HMG-CoA, a substrate of HMGCR.[19] Cholesterol which is an end product of the mevalonate pathway, is utilized as a precursor of several vital bioactive substances, including steroid hormones, vitamin D, oxysterols, and bile acid.[10,20] Excess cholesterol can also be esterified by sterol O-acyl transferase (SOAT, also known as acyl-CoA cholesterol acyltransferase; ACAT) to be stored into lipid droplets, and can also be effluxed through the ATP-binding cassette A1 (ABCA1) or ABCG1, regulating cellular cholesterol content.[20,21,22]

In the present study, we aimed to identify the molecular features related to statin sensitivity in cancer cells using comprehensive gene expression analysis. Our data indicates potential variations in the metabolic nature of statin-sensitive and statin-resistant cancer cells. These findings may provide basic information for the identification of statin-sensitive cancers and the development of novel therapeutic strategies that potentiate the anti-cancer effects of statins.

Materials and Methods

Cell culture

In our previous research, we classified 14 cancer cell lines derived from the NCI-60 line into two groups: in group one, statins were effective (statin-sensitive cancer cells), and in group two statins were ineffective (statin-resistant cancer cells).[8)] Among the statin-sensitive cancer cells, mesenchymal-like human non-small cell lung cancer (NSCLC)-derived HOP-92 cells (undifferentiated, large cell-derived) were the most sensitive to statins. Therefore, this cell line was selected as the statin-sensitive cancer cell line in the present study. For comparison, human NSCLC-derived epithelial-like NCI-H322M cells (small cell bronchoalveolar carcinoma-derived) were used as statin-resistant cancer cells. The NCI-H322M and HOP-92 lung cancer-derived cell lines were obtained from the DCTD Tumor Repository (National Cancer Institute, Frederick, MD, USA). These cell lines were cultured in RPMI 1640 medium (ThermoFisher Scientific, Waltham, MA, USA), supplemented with 10% heat-inactivated fetal bovine serum (FBS, Biosera, Boussens, France) and penicillin/streptomycin (Fujifilm Wako Pure Chemical, Osaka, Japan; final concentration: 100 units/mL penicillin G and 100 μg/mL streptomycin) in a humidified incubator at 37 °C with 5% CO_2.

Atorvastatin (Sigma-Aldrich, St. Louis, MO, USA) was dissolved in dimethyl sulfoxide (DMSO, Fujifilm Wako Pure Chemical). Cells were seeded in 6-well plates at a density of 1×10^5 cells/mL and incubated overnight prior to treatment with 0.1–10 μM atorvastatin for 24 h. Cells treated with 0.1% DMSO were used as vehicle controls.

Rescue test with HMG-CoA

HOP-92 cells were seeded into 96-well plates at a density of 5×10^4 cells/mL and allowed to attach overnight. The cells were then treated with 10 μM atorvastatin alone or in combination with 10–100 μM HMG-CoA (Sigma-Aldrich) for 72 h. Cell viability was determined using the Cell Counting Kit-8 (CCK-8; Dojindo Laboratories, Kumamoto, Japan).

Crystal violet staining

Cells in the 96-well plate were fixed overnight with 10% neutral-buffered formalin (pH 7.4; Fujifilm Wako Pure Chemical). Then, the cells were stained with 0.1% crystal violet (Fujifilm Wako Pure Chemical) in 20% methanol at room temperature for 30 min. The cells were washed with tap water until the unbound dye was completely removed. After air-drying, the crystal violet dye was eluted using 100% methanol. Absorbance at 595 nm was measured using a microplate reader (Sunrise Remote; Tecan Austria GmbH, Grödig, Austria).

RNA extraction

An ISOSPIN Cell & Tissue RNA kit (Nippon Gene, Tokyo, Japan) was used to extract total RNA from cells 24 h after the addition of atorvastatin, in accordance with the manufacturer's instructions.

Real-time reverse transcription polymerase chain reaction (RT-PCR)

The cDNA was synthesized from 1 μg of total RNA using ReverTra Ace qPCR RT Master Mix (Toyobo, Osaka, Japan). The primer sets used for the PCRs are listed in Supplementary Table S1. PCR was performed using a LightCycler FastStart DNA Master^{PLUS} SYBR Green I mix and a LightCycler rapid thermal cycler system (Roche Diagnostics, Lewes, UK). *RPLP1* was used as an endogenous control.

RNA-sequencing and data analysis

Sequencing library construction and subsequent RNA sequencing (RNA-seq) were performed by Macrogen Japan Corp. (Kyoto, Japan) using an Illumina NovaSeq 6000 sequencer with paired ends of 101 bp. FASTq files which were obtained from Macrogen Japan Corp. and subsequent analyses were conducted by the Research Institute of Bio-System Informatics, TOHOKU CHEMICAL Co., Ltd. (Iwate, Japan), as described previously.[23)]

Differential gene expression analysis was conducted using edgeR 3.20.9. The gene lists derived from edgeR included 60,617 genes, and the 1059 differentially expressed genes were selected based on $P < 0.05$ and $\log_2 FC \geq |1|$ (FC denoted the fold-change in the 1 μM statin group vs. the 0 μM statin group). Customized heatmaps of the gene ontology (GO) terms were created using the heatmap.2 package in gplots, including the regulation of cholesterol biosynthetic process (GO:0045540), coenzyme A metabolic process (GO:0015936), and cholesterol homeostasis (GO:0042632). Genes (Ensembl ID) that included each GO were obtained from the org.Hs.eg.db database (https://bioconductor.org/packages/release/data/annotation/html/org.Hs.eg.db.html).

Western blotting

Cells in 6-well plates were washed twice with cold PBS, followed by incubation with CelLytic M solution (Sigma-Aldrich) on ice for 15 min. The subsequent experiment was performed as mentioned previously.[16)] The protein levels (10 μg per lane) of HMGCS1, HMGCR, FDFT1, and GGPS1 were determined using the anti-HMGCS1 rabbit monoclonal

antibody (1:1000 dilution, #36877; Cell Signaling Technology, Beverly, MA, USA), anti-HMGCR mouse monoclonal antibody (1:1000 dilution, AMAb90618; Atlas, Cambridge, UK), anti-FDFT1 mouse monoclonal antibody (1:400 dilution, sc-271602; Santa Cruz Biotechnology, Santa Cruz, CA, USA), and anti-GGPS1 mouse monoclonal antibody (1:400 dilution, sc-271680; Santa Cruz Biotechnology). Anti-glyceraldehyde-3-phosphate dehydrogenase (GAPDH; 14C10) rabbit monoclonal antibody (1:2000 dilution, #2118; Cell Signaling Technology) was used to detect GAPDH as the internal standard. The membranes were then incubated with horseradish peroxidase (HRP)-labeled secondary antibodies (anti-mouse IgG goat antibody; R&D Systems, Minneapolis, MN, USA, or anti-rabbit IgG goat antibody; SeraCare, Milford, MA, USA). The nitrocellulose membrane was washed with Tris buffer and incubated with Clarity Western ECL Substrate Chemiluminescent Detection Reagent (Bio-Rad, CA, USA) for 5 min. Protein signals were detected using a C-DiGit Blot Scanner (Li-Cor Biosciences, Lincoln, NE, USA).

Cholesterol assay

Cholesterol was measured using a Cholesterol Quantitation Kit (Sigma-Aldrich) according to the manufacturer's instructions. The medium was removed 24 h after the addition of atorvastatin or DMSO. The attached cells were washed with PBS and collected in conical tubes using trypsin digestion. The medium was then removed by centrifugation at 200 × g for 5 min. The cells were resuspended in an FBS-free medium and adjusted to a concentration of 1×10^6 cells/mL. One milliliter of the cell suspension was dispensed into three 1.5-mL microfuge tubes such that each tube contained 1×10^6 cells. The cell suspension was centrifuged at 3000 rpm for 5 min and the supernatant was removed. After freezing the pellet at -80 °C, 200 µL of chloroform:isopropanol:Nonidet P-40 (replacement for IGEPAL CA-630) (7:11:0.1) was added to the tubes for cell fracture. The mixture was sonicated for 15 min at 250 W and 4 °C using a sonicator (Bioruptor® UCD-250), with a program setting of 15 s of sonication followed by 15 s interval. After centrifugation at 13,000 × g for 10 min, the supernatant was transferred to a new tube. Chloroform was removed by evaporation at 50 °C using a heat block with the tube lid open. Organic solvent residue was evaporated using a centrifuge evaporator for 30 min. The dried lipid was dissolved with 200 µL of the cholesterol assay buffer, sonicated for 2 min at 4 °C with a program of 15 s sonication at 250 W followed by 15 s intervals and then vortexed. For the experiment, a total volume of the 50 µL per well in a 96-well plate was used. The reaction mixture for total and free cholesterol measurements was prepared according to the

manufacturer's instructions. After adding each reaction mix to each well (50 µL) by pipetting, they were thoroughly mixed. The reaction was incubated for 60 min at 37 °C in dark. The absorbance was measured at 570 nm (A_{570}) using a microplate reader. The free cholesterol value was subtracted from the total cholesterol value to determine the cholesterol ester value.

Metabolite extraction and metabolome analysis using C-SCOPE

The culture medium was aspirated from a 100 mm dish containing atorvastatin-treated and control cancer cells and metabolites were extracted for metabolome analysis. Metabolome analysis was conducted using the C-SCOPE package in HMT. Capillary electrophoresis-time-of-flight mass spectrometry (CE-TOFMS) for cation analysis and CE-tandem mass spectrometry (CE-MS/MS) for anion analysis were performed according to previously described methods.[24,25] Because the sizes of the two cell types were different, normalization was performed using cell number and cell volume (pL). Details have been described previously.[23]

Statistical analyses

Statistical analyses were performed using Excel Statistics 2016 for Windows (version 4.05; SSRI, Tokyo, Japan). Data were compared using Dunnett's *post-hoc* test, Bonferroni *post-hoc* test, and Student's *t*-test with a significance level of $P < 0.05$ (two-tailed).

Results

Treatment with 1 μM atorvastatin had a morphological effect on statin-sensitive cancer cells

In the statin-resistant NCI-H322M cells, no morphological changes were observed on addition of atorvastatin to the growth media at a concentration of 10 μM. However, with respect to the statin-sensitive HOP-92 cells, cell morphology was altered, with cells appearing thinner when treated with 1 μM atorvastatin for 24 h compared with control and 0.1 μM atorvastatin-treated cells (Supplementary Figure S1). Therefore, a concentration of 1 μM atorvastatin was used to identify molecular differences between statin-resistant and statin-sensitive cancer cells.

Basal expression levels of the mevalonate pathway enzymes were low in statin-sensitive cancer cells

First, we assessed the expression patterns of the mevalonate pathway genes with and without atorvastatin treatment. Heat map of "regulation of cholesterol biosynthetic process" showed that in about two thirds of the cholesterol biosynthesis genes, these expressions were lower in HOP-92 cells than that in NCI-H322M cells regardless of atorvastatin treatment (Fig. 1). The basal expression levels of most enzymes in the mevalonate pathway (Fig. 1, black and blue arrows) were lower in HOP-92 cells, except for *LSS* (Lanosterol synthase) and *IDI1* (Isopentenyl-Diphosphate Delta Isomerase 1) (Fig. 1). We further evaluated the fluctuations in mRNA and protein expression after atorvastatin treatment of the selected genes, including *HMGCS1*, *HMGCR*, *FDFT1*, and *GGPS1* (Fig.1, blue arrows; Fig.2A, red letters). Atorvastatin remarkably induced HMGCR protein in HOP-92 and in NCI-H322M cells in a dose-dependent manner (Fig. 2B, Supplementary Figure S2) whereas significant increase in *HMGCR* mRNA were observed only when HOP-92 cells were exposed to 1 μM atorvastatin ($P < 0.05$) (Fig. 2D). Although mRNA levels in both cancer cell lines tended to increase, the increase in mRNA level was gradual compared to that at the protein level. Moreover, *HMGCS1* mRNA significantly increased in the presence of 1 μM atorvastatin in both cell lines ($P < 0.05$) (Fig. 2C) while no obvious increase was detected in the protein level (Fig. 2B, Supplementary Figure S2). *FDFT1* mRNA was dose-dependently reduced by atorvastatin in HOP-92 cells, however not in NCI-H322M cells (Fig. 2E), and no significant changes were observed in protein expression (Fig. 2B, Supplementary Figure S2). Atorvastatin did not affect *GGPS1* mRNA and its protein levels in either cell line (Fig. 2B and F, Supplementary Figure S2).

Basal levels of CoA and HMG-CoA differed between statin-sensitive and statin-resistant cancer cells

CoA metabolism-related factors were then examined as a part of the initial process of the mevalonate pathway. Heatmap of "coenzyme A metabolic process" showed that atorvastatin markedly decreased *PANK2* in the HOP-92 cells, however not in the NCI-H322M cells (Fig. 3A, black arrow). Real-time RT-PCR analysis showed that 0.1 μM atorvastatin significantly reduced *PANK2* mRNA in HOP-92 cells although significant difference was not observed in the group treated with 1 μM atorvastatin (Fig. 3C). However, no alterations in *PANK2* mRNA expression were observed in the NCI-H322M cells (Fig. 3B). We also assessed *PANK2* mRNA levels in prostate cancer cell lines; however, no significant changes were observed in either statin-sensitive PC-3 or statin-resistant DU-145 cells (Supplementary Figure S3A, B). We further evaluated the cellular levels of CoA and HMG-CoA. HMG-CoA levels significantly increased on treatment with 1 μM atorvastatin ($P < 0.05$) and CoA levels tended to increase in NCI-H322M cells (Fig. 4A, B). In the HOP-92 cells, no significant changes in the HMG-CoA and CoA metabolite levels were observed after atorvastatin treatment; however, CoA levels tended to decrease (Fig. 4A, B). Moreover, the basal levels of HMG-CoA and CoA were significantly lower in the HOP-92 cells than in the NCI-H322M cells ($P < 0.01$) (Fig. 4A, B). To investigate whether differences in CoA levels cause variations in statin sensitivity, we performed a rescue test with HMG-CoA supplementation. However, even a high dose of HMG-CoA, which reduced cell viability, did not rescue HOP-92 cells from the growth-inhibitory effect of atorvastatin (Fig. 4C, D).

Atorvastatin decreased expression of sterol esterification enzyme *SOAT1* in statin-sensitive cancer cells

We analyzed expression patterns of genes belonging to GO term "cholesterol homeostasis" as a process following the mevalonate pathway (Fig 5A). Overall, gene expression patterns differed greatly between statin-sensitive and statin-resistant cancer cells. In addition, some genes showed different alteration tendencies after atorvastatin treatment between HOP-92 cells and NCI-H322M cells. Among these, we focused on the sterol esterification enzyme, *SOAT1*, which regulates cholesterol storage (Fig 5A, black arrow). Real-time RT-PCR revealed that *SOAT1* mRNA significantly reduced by treatment with low dose of atorvastatin (0.1 μM) in HOP-92 cells ($P < 0.05$) whereas even high dose atorvastatin treatment (10 μM) did not cause any change in *SOAT1* expression in NCI-H322M cells (Fig. 5B, C). Similar effects have been observed in prostate cancer cell lines. Although atorvastatin downregulated *SOAT1* mRNA expression in statin-sensitive PC-3 cells in a dose-dependent manner, no alterations were observed in statin-resistant DU-145 cells (Supplementary Figure S3C, D).

Atorvastatin reduced the ratio of cholesterol ester to total cholesterol in statin-sensitive cancer cells

We measured the levels of free and esterified forms of cholesterol due to decreased *SOAT1* expression in HOP-92 cells. In NCI-H322M cells, no changes were observed in free cholesterol, cholesterol ester, and total cholesterol when treated with 1 μM atorvastatin (Fig. 6A–C, left panels). However, HOP-92 cells showed significant reductions in cholesterol ester and total cholesterol in response to 1 μM atorvastatin treatment and free cholesterol levels were not altered (Fig. 6A–C, right panels). In addition, 1 μM atorvastatin markedly decreased the ratio of cholesterol ester to total cholesterol in HOP-92 cells (Fig. 6D, right panels). On the contrary, in the NCI-H322M cells, the ratio of cholesterol ester to total cholesterol did not change even when free cholesterol decreased on treatment with 10 μM atorvastatin (Fig. 6B, D, left panels).

Combination of atorvastatin and SOAT1 inhibitor showed additive growth inhibitory effect in NCI-H322M cells

Cholesterol quantification showed differences in the effect of atorvastatin with respect to cholesterol storage between statin-sensitive and statin-resistant cancer cells. Therefore, we examined the growth inhibitory effect of atorvastatin with or without the SOAT1 inhibitor, avasimibe. Atorvastatin (30 μM) and avasimibe (10 μM) both decreased cell viability by 22% and 20% respectively in the NCI-H322M cells (Fig. 7B). A combination of both showed a greater reduction in cell viability (34%) (Fig. 7B). Additionally, atorvastatin caused marked cell aggregation in the presence and absence of avasimibe (Fig. 7A).

Discussion

Previous studies have demonstrated the relationship between the expression of mevalonate pathway-related enzymes and statin sensitivity in several types of cancer cells. Kimbung *et al.* reported that atorvastatin-sensitive breast cancer cells showed lower basal levels of cholesterol biosynthesis gene expression than atorvastatin-less sensitive cells.[15] In addition, other studies showed a correlation between statin-induced upregulation levels of HMGCR protein and statin sensitivity in breast cancer and multiple myeloma.[12,14,15] Similar to the cellular characteristics of breast cancer cells with respect to statin sensitivity reported by Kimbung *et al.*, we also found that basal gene expression of most cholesterol biosynthesis enzymes in lung cancer was lower in statin-sensitive HOP-92 cells than in statin-resistant NCI-H322M cells (Fig. 1). This implies that statin-sensitive cancer cells originally have a lower levels of mevalonate pathway activity regardless of the cell type. On the contrary, HMGCR protein increase after treatment with 1 μM atorvastatin was similar in both HOP-92 and NCI-H322M cells (Fig. 2B, Supplementary Figure S2), suggesting that statin-sensitive cancer cells also exhibit an allostatic response to statin treatment.

The anti-cancer effects of statins are attributed to the depletion of farnesyl pyrophosphate (FPP) and GGPP.[6,26–28] In addition, some squalene synthase (FDFT1) inhibitors have been reported to increase cellular FPP and GGPP levels.[29,30] Therefore, we first hypothesized that atorvastatin differently affects the expressions of *GGPS1* and *FDFT1* depending on statin sensitivity. However, atorvastatin did not affect GGPS1 mRNA or protein levels (Fig. 2B, F, Supplementary Figure S2). Although we showed that atorvastatin decreased *FDFT1* mRNA levels only in HOP-92 cells, further investigation is needed to understand the biological significance of these results and whether alteration of *FDFT1* mRNA levels is directly related to statin sensitivity (Fig. 2B, E, Supplementary Figure S2). Xu *et al.* demonstrated that *GGPS1* expression may be correlated with pitavastatin sensitivity in oral and esophageal cancer cells.[31] Similarly, our data showed that basal *GGPS1* expression was lower in statin-sensitive lung cancer cells than in statin-resistant lung cancer cells (Fig. 1). These observations suggest that *GGPS1* expression can be used as a biomarker to predict statin sensitivity across cancer origins.

Because statins reversibly inhibit HMGCR activity by competing with HMG-CoA,[32] the substrate concentration could affect the inhibitory potency of statins against HMGCR.[33] In the present study, we showed that statin-sensitive cancer cells had a low CoA and HMG-CoA content (Fig. 4A, B). This suggests that the amount of substrate available for the mevalonate pathway is limited in statin-sensitive cancer cells. However, we found that HMG-CoA did not reverse the growth-inhibitory effect of atorvastatin (Fig. 4D). We and others have demonstrated

that mevalonate supplementation could rescue cancer cells from statin-induced cell death and growth reduction.[6,26–28] Taken together, lack of not an HMGCR substrate but HMGCR product may be responsible for the statin-sensitive phenotype in cancer cells. Thus, differences in the amounts and activities of HMGCR are likely to reflect differences in statin sensitivity.

CoA is synthesized from pantothenate (vitamin B_5) via several enzymatic reactions, including the rate-limiting enzyme, PANK.[19] Our data showed that atorvastatin may affect CoA synthesis by decreasing *PANK2* expression in statin-sensitive HOP-92 cells (Fig. 3A, C, and 4B). In patients suffering from pancreatic cancer, *PANK2* is reported to be upregulated in the peripheral blood when compared to the participants in the healthy group[34] and a study showed that *PANK2* silencing reduced the cell number in several types of cancer cell lines.[35] Another study reported that high *PANK2* expression was correlated with long-term survival in patients with acute myeloid leukema.[36] These observations suggest that *PANK2* may have both positive and negative effects on cancer progression. In this study, we showed that treatment with atorvastatin slightly decreased *PANK2* expression in the HOP-92 cells, whereas no change was observed in the PC-3 cells, a statin-sensitive cancer cell line. This suggests that the responsiveness of *PANK2* to statin treatment differs depending on the cancer cell types.

Cholesterol esterification enzyme SOAT1 catalyzes conversion of excess free cholesterol into cholesterol ester to avoid toxicity of increased cholesterol.[22] Here, we found that atorvastatin decreases *SOAT1* expression and suppresses cholesterol esterification in statin-sensitive HOP-92 cells. Santos *et al.* reported that atorvastatin reduced SOAT1 protein levels in the presence of cisplatin in the atorvastatin-sensitive breast cancer cell line MDA-MB-231, although atorvastatin alone did not change SOAT1 expression.[37] These observations suggest the potential effect of atorvastatin in decreasing SOAT1 expression in statin-sensitive cancer cells, with some differences depending on the cancer origin. Moreover, *SOAT1* expression and cholesterol esterification levels were not affected by treatment with atorvastatin in statin-resistant NCI-H322M cells, unlike those in the HOP-92 cells (Fig. 5 and 6D). This suggests that the stability of the cholesterol storage process for atorvastatin may differ between statin-sensitive and statin-resistant cancer cells. Zhu *et al.* demonstrated that *SOAT1* silencing and SOAT1 inhibition downregulate cholesterol metabolism-related genes, including HMGCR, in gastric cancer.[38] Therefore, we investigated whether SOAT1 mediates statin resistance in NCI-H322M cells by supporting the mevalonate pathway. Although combination of atorvastatin and the SOAT1 inhibitor avasimibe showed an additive growth reduction in NCI-H322M cells, avasimibe did not seem to strongly enhance the growth inhibitory effect of statins (Fig. 7). This suggests that SOAT1 may not be a leading factor in statin resistance.

Our findings are summarized in schematic diagrams (Fig. 8). Thus, we identified the features of statin-sensitive cancer cells that originally had low activity in the cholesterol synthesis pathway and had a low CoA content. In addition, we also found different reactivities of CoA synthesis and cholesterol storage processes in response to atorvastatin treatment between statin-sensitive and statin-resistant cancer cells, represented by fluctuations in *PANK2* and *SOAT1* expression. These metabolic variations may provide useful information for developing predictive factors for statin-sensitive cancer and combination therapy with statins. Although this study demonstrated the metabolic nature of cancer cells based on statin sensitivity, we could not determine whether these features directly mediate statin sensitivity. Further investigations are required to clarify these limitations.

Acknowledgements

The authors would like to thank Takahiro Nakayama from the Research Institute of Bio-System Informatics, TOHOKU CHEMICAL CO., LTD., and Yuta Horiuchi from Human Metabolome Technologies, Inc. (HMT) for their help with the transcriptome and metabolome analyses in this study. We would like to thank Editage (www.editage.com) for English language editing.

Conflict of Interest

The authors declare no conflict of interest.

Authors' contributions

J.T., T.W. and K.W. designed the experiments. J.T., T.W., A.S., K.M., T.I. and K.W. performed the experiments. J.T., T.W. and K.W. analyzed the data. J.T., T.W. and K.W. wrote the manuscript. All authors have read the manuscript and approved its final version.

Funding information

This research was financially supported by a JSPS KAKENHI Grant #JP19K23926 in Grant-in-Aid for Research Activity Start-up, a JSPS KAKENHI Grant #JP20K07666 in a Grant-in-Aid for Scientific Research (C), and a JSPS KAKENHI Grant # JP19H03514 in a Grant-in-Aid for Scientific Research (B).

This article contains Supplementary Materials.

References

1) Elis A. Current and future options in cholesterol lowering treatments. *Eur. J. Intern. Med.*, **112**, 1–5 (2023).
2) Michaeli DT, Michaeli JC, Albers S, Boch T, Michaeli T. Established and Emerging Lipid-Lowering Drugs for Primary and Secondary Cardiovascular Prevention. *Am. J. Cardiovasc. Drugs*, **23**, 477–495 (2023).
3) Jiang P, Mukthavaram R, ChaoY, Nomura N, Bharati IS, Fogal V, Pastorino S, Teng D, Cong X, Pingle SC, Kapoor S, Shetty K, Aggrawal A, Vali S, Abbasi T, Chien S, Kesari S. In vitro and in vivo anticancer effects of mevalonate pathway modulation on human cancer cells. *Br. J. Cancer*, **111**, 1562–1571 (2014).
4) Alizadeh J, Zeki AA, Mirzaei N, Tewary S, Moghadam AR, Glogowska A, Nagakannan P, Eftekharpour E, Wiechec E, Gordon JW, Xu FY, Field JT, Yoneda KY, Kenyon NJ, Hashemi M, Hatch GM, Hombach-Klonisch S, Klonisch T, Ghavami S. Mevalonate Cascade Inhibition by Simvastatin Induces the Intrinsic Apoptosis Pathway via Depletion of Isoprenoids in Tumor Cells. *Sci. Rep.*, **7**, 44841 (2017).
5) Chen MC, Tsai YC, Tseng JH, Liou JJ, Horng S, Wen HC, Fan YC, Zhong WB, Hsu SP. Simvastatin Inhibits Cell Proliferation and Migration in Human Anaplastic Thyroid Cancer. *Int. J. Mol. Sci.*, **18**, 2690 (2017).
6) Ishikawa T, Hosaka YZ, Beckwitt C, Wells A, Oltvai ZN, Warita K. Concomitant attenuation of HMG-CoA reductase expression potentiates the cancer cell growth-inhibitory effect of statins and expands their efficacy in tumor cells with epithelial characteristics. *Oncotarget*, **9**, 29304–29315 (2018).
7) Jiao Z, Cai H, Long Y, Sirka OK, Padmanaban V, Ewald AJ, Devreotes PN. Statin-induced GGPP depletion blocks macropinocytosis and starves cells with oncogenic defects. *Proc. Natl. Acad. Sci. U. S. A.*, **117**, 4158–4168 (2020).
8) Warita K, Warita T, Beckwitt CH, Schurdak ME, Vazquez A, Wells A, Oltvai ZN. Statin-induced mevalonate pathway inhibition attenuates the growth of mesenchymal-like cancer cells that lack functional E-cadherin mediated cell cohesion. *Sci. Rep.*, **4**, 7593 (2014).
9) Raghu VK, Beckwitt CH, Warita K, Wells A, Benos PV, Oltvai ZN. Biomarker identification for statin sensitivity of cancer cell lines. *Biochem. Biophys. Res. Commun.*, **495**, 659–665 (2018).

10) Guerra B, Recio C, Aranda-Tavío H, Guerra-Rodríguez M, García-Castellano JM, Fernández-Pérez L. The Mevalonate Pathway, a Metabolic Target in Cancer Therapy. *Front. Oncol.*, **11**, 626971 (2021).
11) Casella C, Miller DH, Lynch K, Brodsky AS. Oxysterols synergize with statins by inhibiting SREBP-2 in ovarian cancer cells. *Gynecol. Oncol.*, **135**, 333–341 (2014)
12) Göbel A, Breining D, Rauner M, Hofbauer LC, Rachner TD. Induction of 3-hydroxy-3-methylglutarylCoA reductase mediates statin resistance in breast cancer cells. *Cell Death Dis.*, **10**, 91 (2019).
13) Longo J, Mullen PJ, Yu R, van Leeuwen JE, Masoomian M, Woon DTS, Wang Y, Chen EX, Hamilton RJ, Sweet JM, van der Kwast TH, Fleshner NE, Penn LZ. An actionable sterol-regulated feedback loop modulates statin sensitivity in prostate cancer. *Mol. Metab.*, **25**, 119–130 (2019).
14) Clendening JW, Pandyra A, Li Z, Boutros PC, Martirosyan A, Lehner R, Jurisica I, Trudel S, Penn LZ. Exploiting the mevalonate pathway to distinguish statin-sensitive multiple myeloma. *Blood*, **115**, 4787–4797 (2010).
15) Kimbung S, Lettiero B, Feldt M, Bosch A, Borgquist S. High expression of cholesterol biosynthesis genes is associated with resistance to statin treatment and inferior survival in breast cancer. *Oncotarget*, **7**, 59640–59651 (2016).
16) Warita K, Ishikawa T, Sugiura A, Tashiro J, Shimakura H, Hosaka YZ, Ohta KI, Warita T, Oltvai ZN. Concomitant attenuation of HMGCR expression and activity enhances the growth inhibitory effect of atorvastatin on TGF-β-treated epithelial cancer cells. *Sci. Rep.*, **11**, 12763 (2021).
17) van Leeuwen JE, Ba-Alawi W, Branchard E, Cruickshank J, Schormann W, Longo J, Silvester J, Gross PL, Andrews DW, Cescon DW, Haibe-Kains B, Penn LZ, Gendoo DMA. Computational pharmacogenomic screen identifies drugs that potentiate the anti-breast cancer activity of statins. *Nat. Commun.*, **13**, 6323 (2022)
18) Irie N, Mizoguchi K, Warita T, Nakano M, Sasaki K, Tashiro J, Osaki T, Ishikawa T, Oltvai ZN, Warita K. Repurposing of the Cardiovascular Drug Statin for the Treatment of Cancers: Efficacy of Statin–Dipyridamole Combination Treatment in Melanoma Cell Lines. *Biomedicines*, **12**, 698 (2024).
19) Czumaj A, Szrok-Jurga S, Hebanowska A, Turyn J, Swierczynski J, Sledzinski T, Stelmnka E. The Pathophysiological Role of CoA. *Int. J. Mol. Sci.*, **21**, 9057 (2020)

20) Centonze G, Natalini D, Piccolantonio A, Salemme V, Morellato A, Arina P, Riganti C, Defilippi P. Cholesterol and Its Derivatives: Multifaceted Players in Breast Cancer Progression. *Front. Oncol.*, **12**, 906670 (2022).
21) Bauer R, Brüne B, Schmid T. Cholesterol metabolism in the regulation of inflammatory responses. *Front. Pharmacol.*, **14**, 1121819 (2023).
22) Tu T, Zhang H, Xu H. Targeting sterol-O-acyltransferase 1 to disrupt cholesterol metabolism for cancer therapy. *Front. Oncol.*, **13**, 1197502 (2023).
23) Warita T, Irie N, Zhou Y, Tashiro J, Sugiura A, Oltvai ZN, Warita K. Alterations in the omics profiles in mevalonate pathway-inhibited cancer cells. *Life Sci.*, **312**, 121249 (2023).
24) Ohashi Y, Hirayama A, Ishikawa T, Nakamura S, Shimizu K, Ueno Y, Tomita M, Soga T. Depiction of metabolome changes in histidine-starved Escherichia coli by CE-TOFMS. *Mol. Biosyst.*, **4**, 135–147 (2008).
25) Ooga T, Sato H, Nagashima A, Sasaki K, Tomita M, Soga T, Ohashi Y. Metabolomic anatomy of an animal model revealing homeostatic imbalances in dyslipidaemia. *Mol. Biosyst.*, **7**, 1217–1223 (2011).
26) Xia Z, Tan MM, Wong WW, Dimitroulakos J, Minden MD, Penn LZ. Blocking protein geranylgeranylation is essential for lovastatin-induced apoptosis of human acute myeloid leukemia cells. *Leukemia*, **15**, 1398–1407 (2001).
27) Wang T, Seah S, Loh X, Chan CW, Hartman M, Goh BC, Lee SC. Simvastatin-induced breast cancer cell death and deactivation of PI3K/Akt and MAPK/ERK signalling are reversed by metabolic products of the mevalonate pathway. *Oncotarget*, **7**, 2532–2544 (2016).
28) Kany S, Woschek M, Kneip N, Sturm R, Kalbitz M, Hanschen M, Relja B. Simvastatin exerts anticancer effects in osteosarcoma cell lines via geranylgeranylation and c-Jun activation. *Int. J. Oncol.*, **52**, 1285–1294 (2018).
29) Wasko BM, Smits JP, Shull LW, Wiemer DF, Hohl RJ. A novel bisphosphonate inhibitor of squalene synthase combined with a statin or a nitrogenous bisphosphonate in vitro. *J. Lipid Res.*, **52**, 1957–1964 (2011).
30) Suzuki N, Ito T, Matsui H, Takizawa M. Anti-inflammatory and cytoprotective effects of a squalene synthase inhibitor, TAK-475 active metabolite-I, in immune cells simulating mevalonate kinase deficiency (MKD)-like condition. *Springerplus*, **5**, 1429 (2016).

31) Xu B, Muramatsu T, Inazawa J. Suppression of MET Signaling Mediated by Pitavastatin and Capmatinib Inhibits Oral and Esophageal Cancer Cell Growth. *Mol. Cancer Res.*, **19**, 585–597 (2021).
32) Istvan ES. Structural mechanism for statin inhibition of 3-hydroxy-3-methylglutaryl coenzyme A reductase. *Am. Heart J.*, **144**, S27–32 (2002).
33) Harrad LE, Bourais I, Mohammadi H, Amine A. Recent Advances in Electrochemical Biosensors Based on Enzyme Inhibition for Clinical and Pharmaceutical Applications. *Sensors*, **18**, 164 (2018).
34) Chen Q, Guo Q, Wang D, Zhu S, Wu D, Wang Z, Lu Y. Diagnosis and prognosis of pancreatic cancer with immunoglobulin heavy constant delta blood marker. *J. Cancer Res. Clin. Oncol.*, **149**, 12977–12992 (2023).
35) Poli M, Derosas M, Luscieti S, Cavadini P, Campanella A, Verardi R, Finazzi D, Arosio P. Pantothenate kinase-2 (Pank2) silencing causes cell growth reduction, cell-specific ferroportin upregulation and iron deregulation. *Neurobiol. Dis.*, **39**, 204–210 (2010).
36) Liu Y, Cheng Z, Li Q, Pang Y, Cui L, Qian T, Quan L, Dai Y, Jiao Y, Zhang Z, Ye X, Shi J, Fu L. Prognostic significance of the PANK family expression in acute myeloid leukemia. *Ann. Transl. Med.*, **7**, 261 (2019).
37) Santos DZD, Guimaraes IDS, Hakeem-Sanni MF, Cochran BJ, Rye KA, Grewal T, Hoy AJ, Rangel LBA. Atorvastatin improves cisplatin sensitivity through modulation of cholesteryl ester homeostasis in breast cancer cells. *Discov. Oncol.*, **13**, 135 (2022).
38) Zhu T, Wang Z, Zou T, Xu L, Zhang S, Chen Y, Chen C, Zhang W, Wang S, Ding Q, Xu G. SOAT1 Promotes Gastric Cancer Lymph Node Metastasis Through Lipid Synthesis. *Front. Pharmacol.*, **12**, 769647 (2021).

Figures and Legends

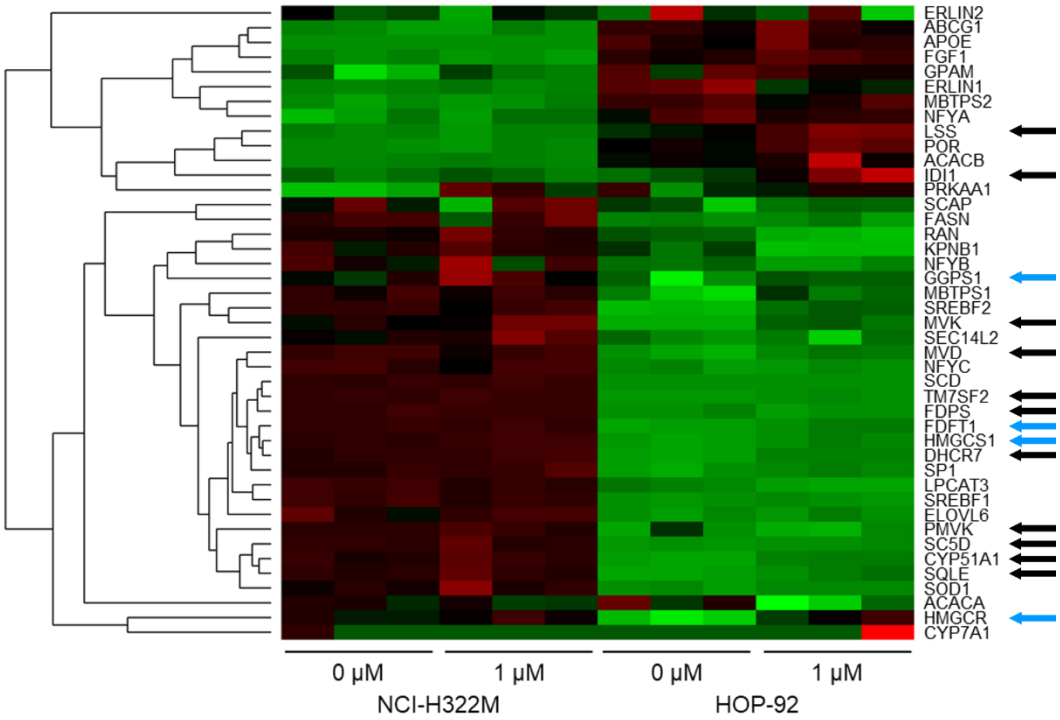

Fig. 1. Custom heatmap of the mevalonate pathway-related genes after atorvastatin treatment in statin-resistant NCI-H322M and statin-sensitive HOP-92 cells

Custom heatmaps of "regulation of cholesterol biosynthetic process" (GO:0045540). Row: sample; Column: gene. Data were represented using the z-score (the relative expression level of a gene in each sample). Red indicates higher level of genes and green indicates lower level of genes. Heatmaps show that statin treatment alters gene expression and that there are remarkable differences in basal gene expression between cells. Black and blue arrows indicate mevalonate pathway enzyme genes. Blue arrows indicate the selected upstream (*HMGCS1* and *HMGCR*) and downstream (*FDFT1* and *GGPS1*) genes in the mevalonate pathway.

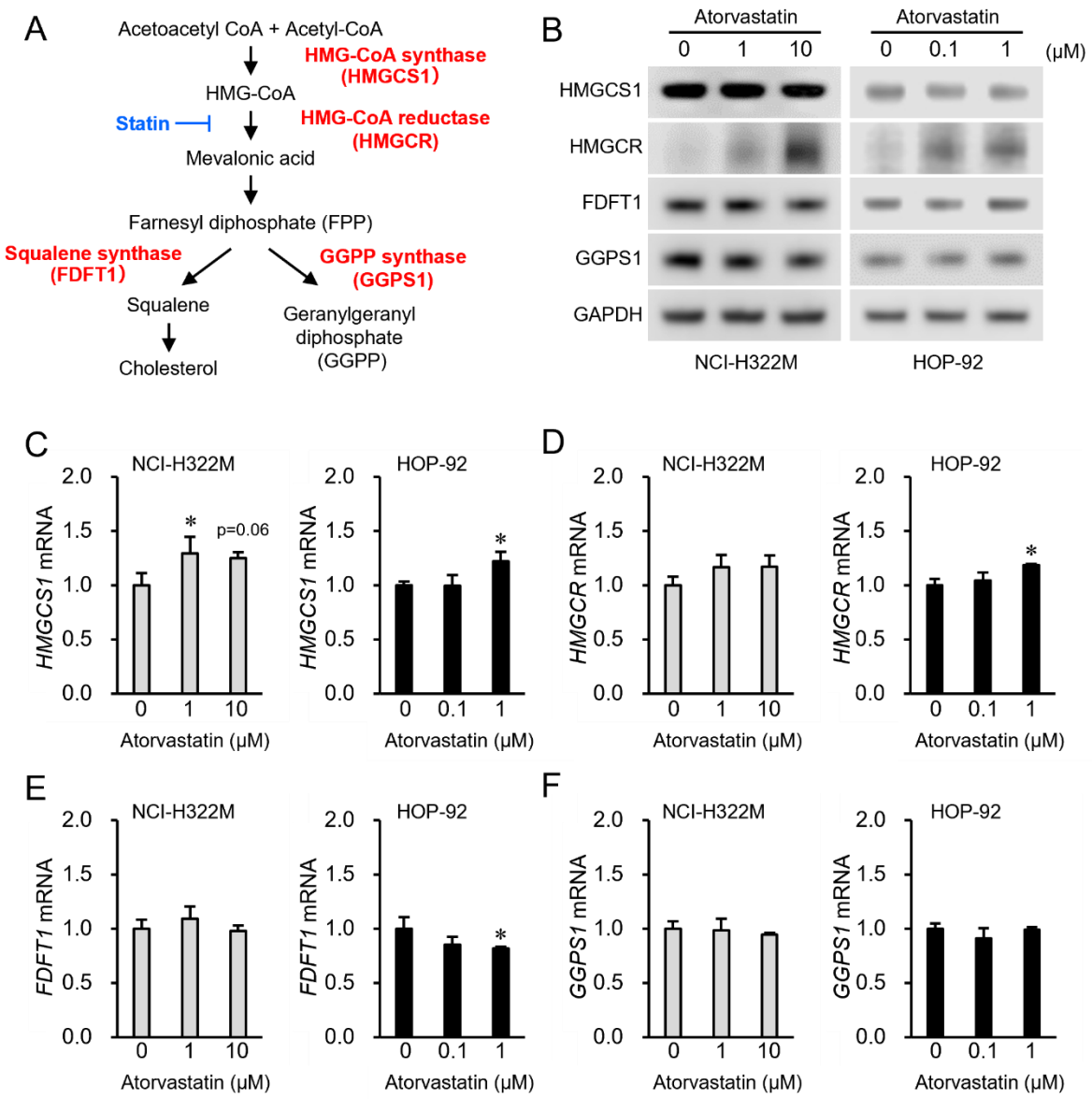

Fig. 2. The mRNA and protein expression levels of enzymes in the mevalonate pathway in statin-resistant NCI-H322M and statin-sensitive HOP-92 cells treated with atorvastatin for 24 h

(A) Schematic view of the mevalonate pathway. Enzymes evaluated using real-time RT-PCR and western blot are shown in red and HMG-CoA reductase inhibitor is shown in blue. (B) Western blot analysis of the expression of HMGCS1, HMGCR, FDFT1, and GGPS1 in the atorvastatin-treated NCI-H322M and HOP-92 cells. GAPDH expression is used as the loading control. Representative images from three independent experiments are shown. Real-time PCR analyses of expression of (C) *HMGCS1*, (D) *HMGCR*, (E) *FDFT1*, and (F) *GGPS1* in statin-resistant NCI-H322M and statin-sensitive HOP-92 cells treated with atorvastatin. Data of real-time RT-PCR are normalized to *RPLP1* levels in each sample and expressed as values relative

to those of the internal control. Data represents mean ± standard deviation (n = 3). Measurement values in each group are compared using the Dunnett's test. *$P < 0.05$.

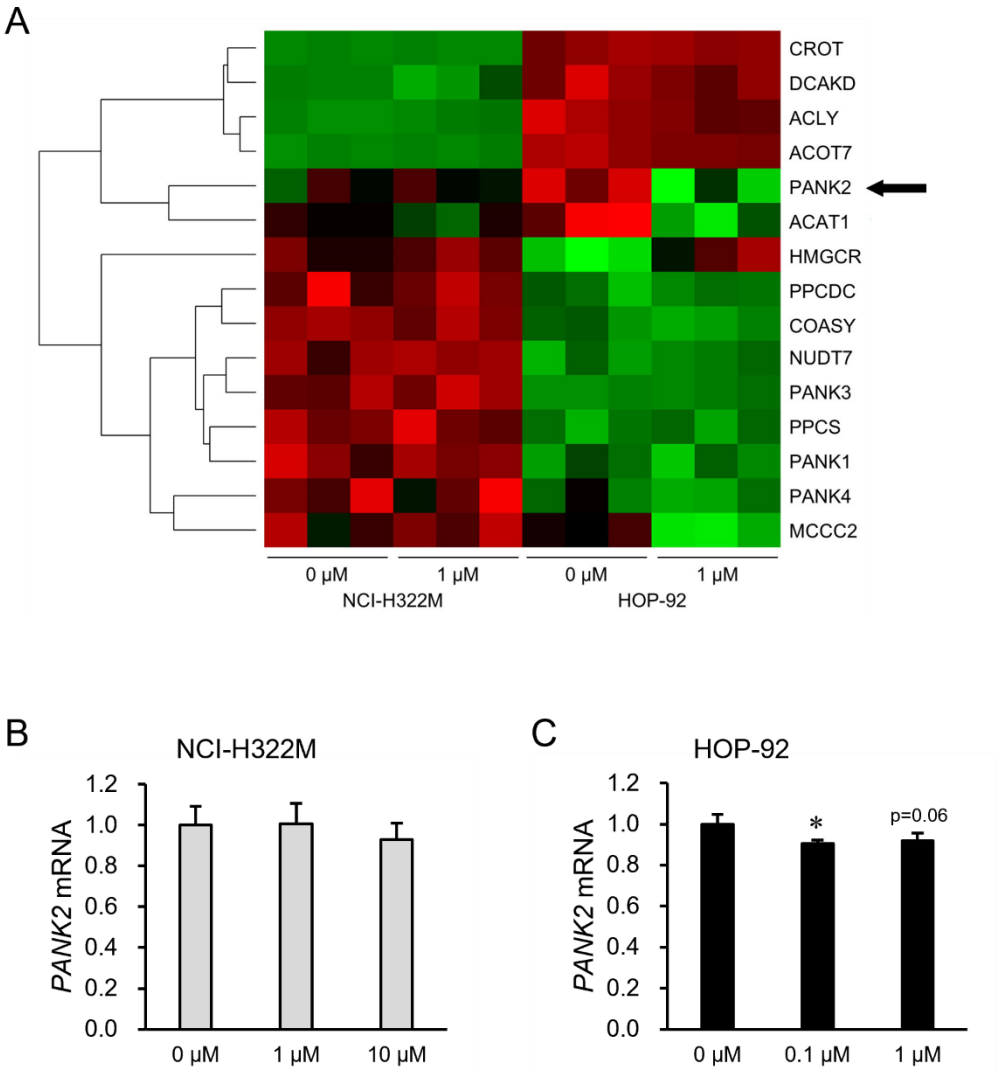

Fig. 3. Custom heatmap of CoA-related genes and the gene expression levels of selected genes after atorvastatin treatment in statin-resistant NCI-H322M and statin-sensitive HOP-92 cells

(A) Custom heatmap of "coenzyme A metabolic process" (GO:0015936). Row: sample; Column: gene. Data were represented using the z-score (relative expression level of a gene between each sample). Red indicates higher level of genes, and green indicates lower level of genes. Heatmaps show that statin treatment alters gene expression and that there are significant differences between cells. Black arrows indicate genes whose expression was altered greatly due to the effect of statins. Real-time PCR analyses data of expression of *PANK2* (B and C) in statin-resistant NCI-H322M and statin-sensitive HOP-92 cells treated with atorvastatin for 24 h. Data of real-time RT-PCR are normalized to *RPLP1* levels in each sample and expressed as values relative to those of the internal control. Each value is shown as mean ± standard

deviation (n = 3). Measurement values for each group are compared using the Dunnett's test. *$P < 0.05$.

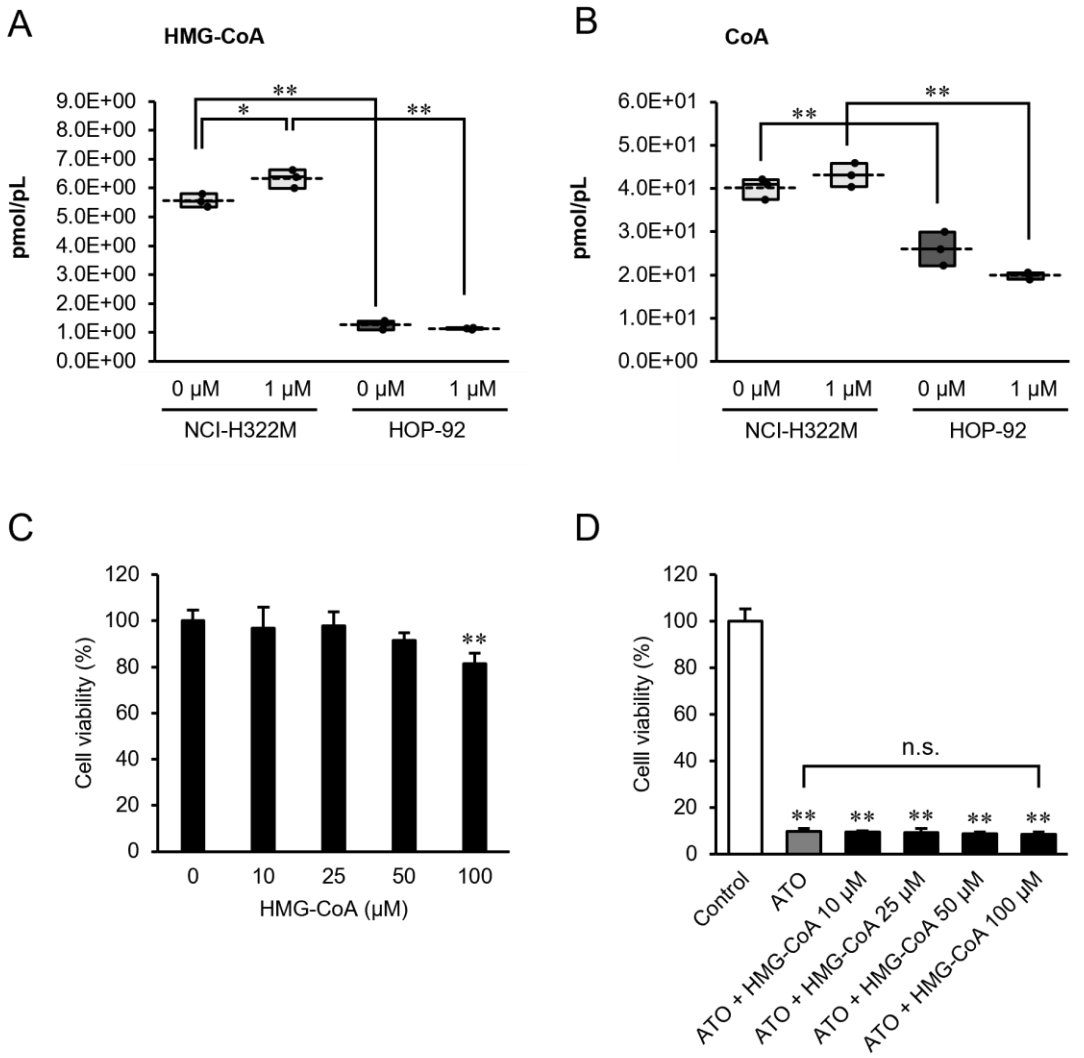

Fig. 4. The box plot of CoA-related metabolite concentrations of statin-resistant NCI-H322M and statin-sensitive HOP-92 cells treated with atorvastatin for 24 h and rescue test with HMG-CoA in HOP-92 cells

The metabolite concentrations (pmol/pL) of (A) HMG-CoA and (B) CoA. Data are shown as mean ± standard deviation (n = 3). The measurement values in each group were compared using the Bonferroni *post-hoc* test. **P* < 0.05, ***P* < 0.01. (C) Cell viability of HOP-92 treated with HMG-CoA alone for 72 h. Data represents mean ± standard deviation (n = 5). The measured values in each group were compared using Dunnett's test. ***P* < 0.01. (D) Effect of HMG-CoA supplementation on atorvastatin-induced growth reduction. HOP-92 cells were treated with 10 μM atorvastatin with or without HMG-CoA for 72 h. Viability is represented as relative value to vehicle control group. Mean ± standard deviation (n = 3). Data were compared using the Bonferroni *post-hoc* test. n.s. not significant, ***P* < 0.01.

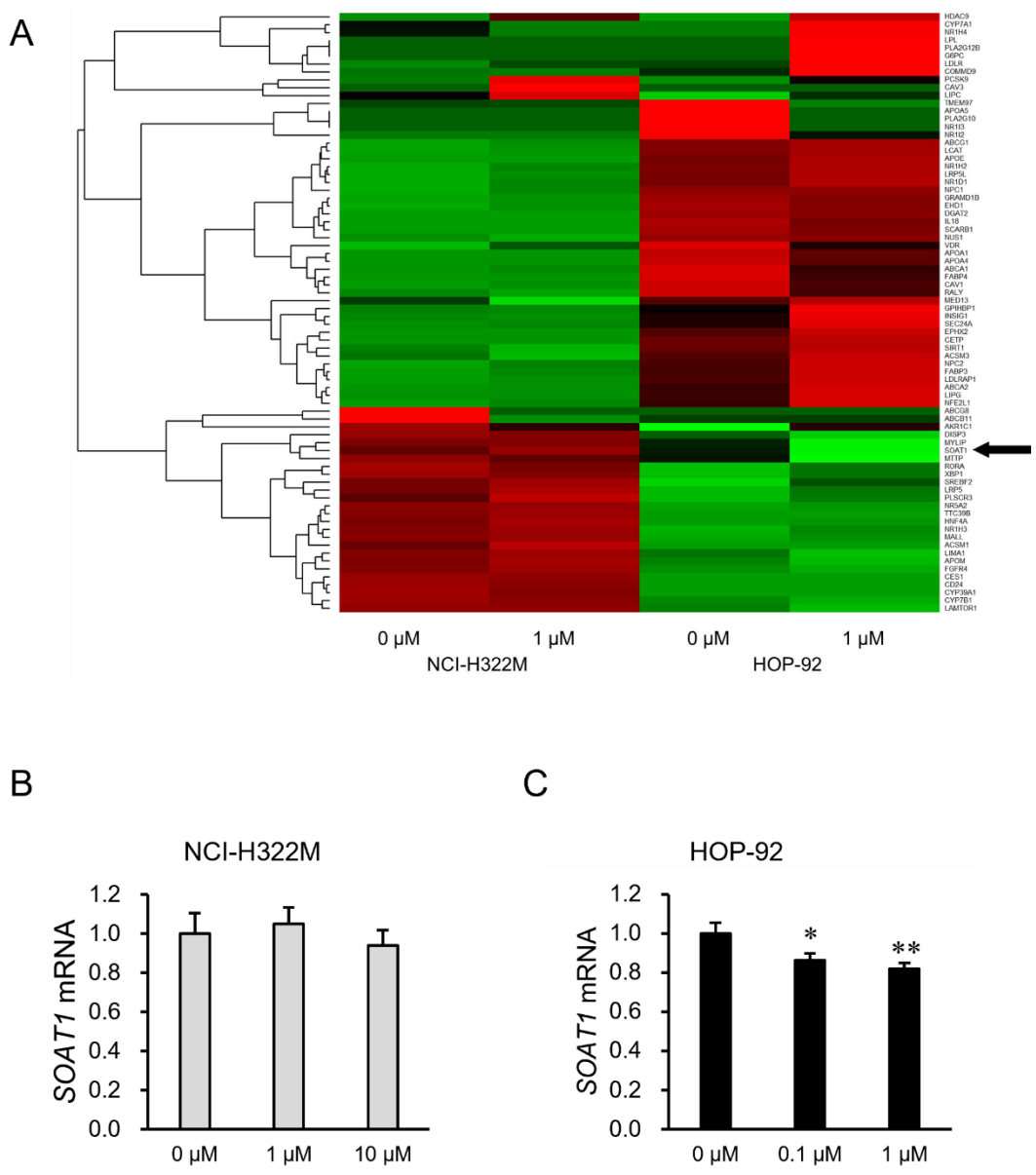

Fig. 5. Custom heatmap of cholesterol metabolism-related genes and the gene expression levels of selected genes after atorvastatin treatment in statin-resistant NCI-H322M and statin-sensitive HOP-92 cells

(A) Custom heatmap of "cholesterol homeostasis" (GO:0042632). Row: group; Column: genes Data is represented using the z-score (relative expression level of a gene between each sample). Red indicates higher level of genes and green indicates lower level of genes. Heatmaps show that statin treatment alters gene expression and that there are significant differences between cells. Black arrow indicates the gene whose expression was altered remarkably due to the effect of statins. Real-time PCR analyses data of expression of *SOAT1* in statin-resistant NCI-H322M cells (B) and statin-sensitive HOP-92 cells (C) treated with atorvastatin for 24 h. Data obtained from real-time RT-PCR were normalized to *RPLP1* levels in each sample and expressed as

values relative to those of the internal control. Each values represent mean ± standard deviation (n = 3). Measurement values for each group are compared using the Dunnett's test. *$P < 0.05$, **$P < 0.01$.

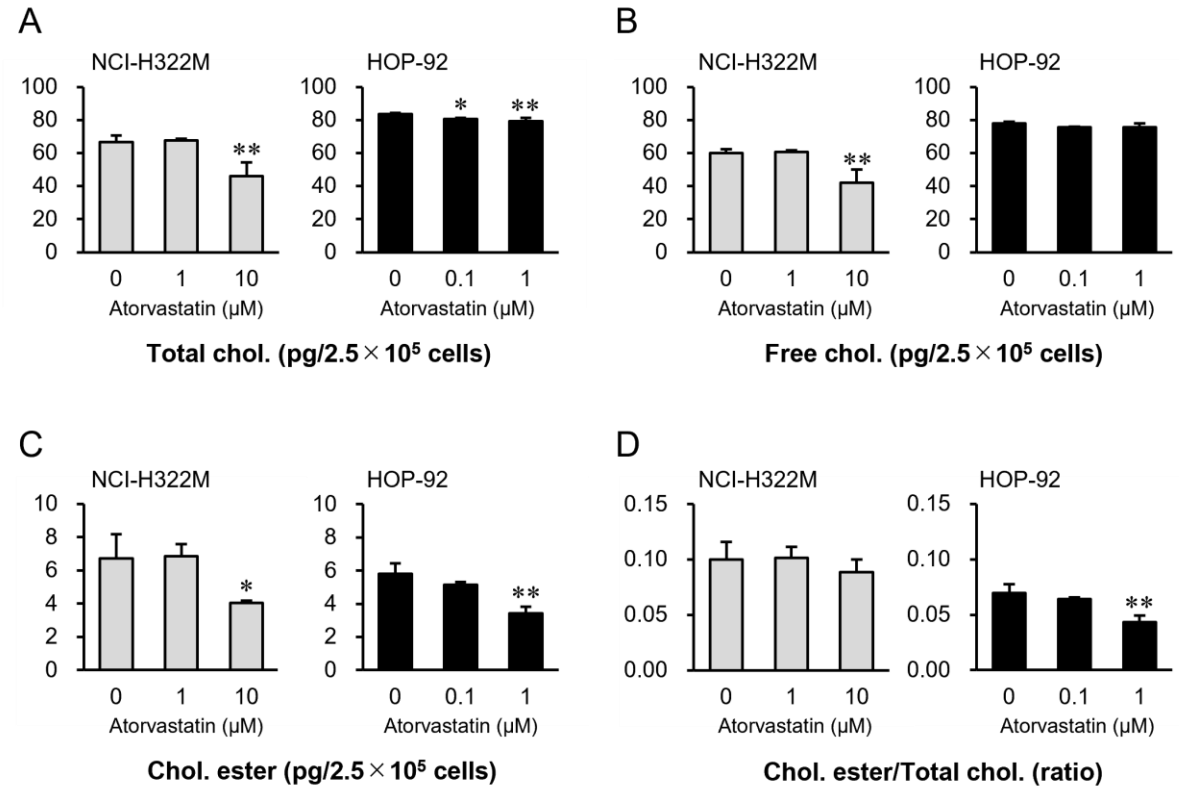

Fig. 6. Effect of atorvastatin on cholesterol levels in statin-resistant NCI-H322M cells and statin-sensitive HOP-92 cells

The levels of total cholesterol (A), free cholesterol (B), cholesterol ester (C), and the ratio of cholesterol ester to total cholesterol (D) were evaluated 24 h after treatment with atorvastatin. Each value represents mean ± standard deviation (n = 3). The values obtained for the experimental group were compared with those obtained for the control group using Dunnett's test. **P* < 0.05, ***P* < 0.01, with respect to each control group.

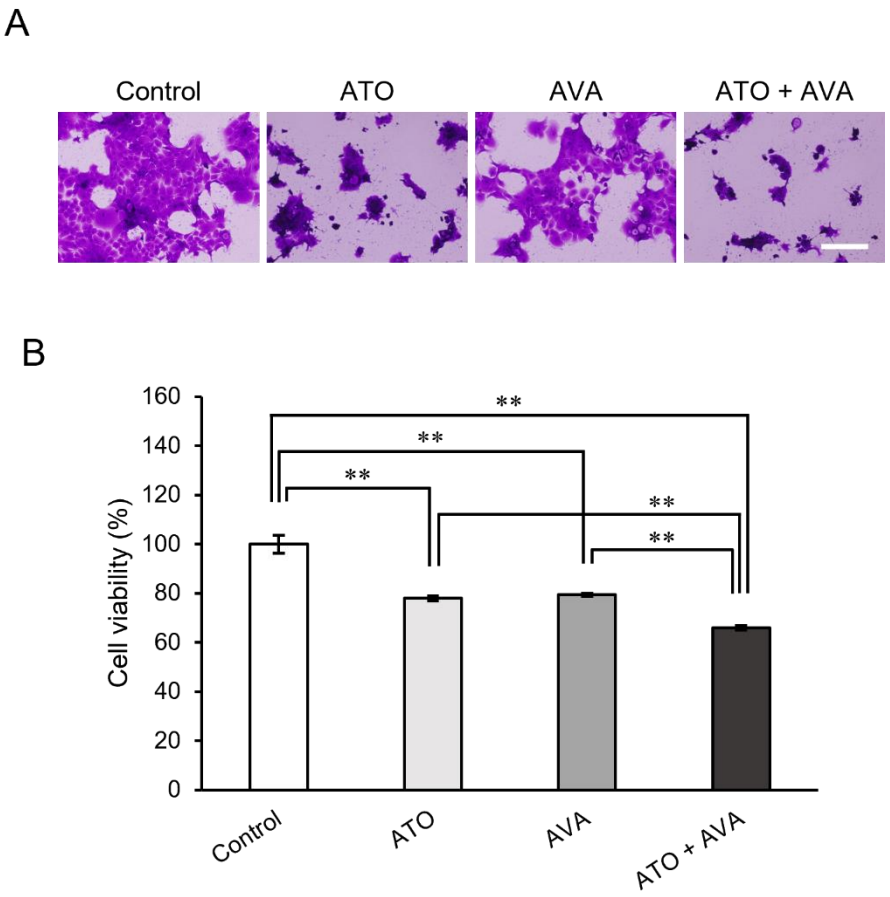

Fig. 7. Combination effect of atorvastatin and avasimibe on viability of statin-resistant NCI-H322M cells

NCI-H322M cells were treated with 30 μM atorvastatin and 10 μM avasimibe for 72 h. (A) Morphology and (B) viability of NCI-H322M cells were evaluated by crystal violet staining. Viability of the vehicle (DMSO)-treated group was set to 100%. Mean ± standard deviation, n = 3, Bonferroni *post-hoc* test., $^{**}P < 0.01$. Scale bar = 200 μm.

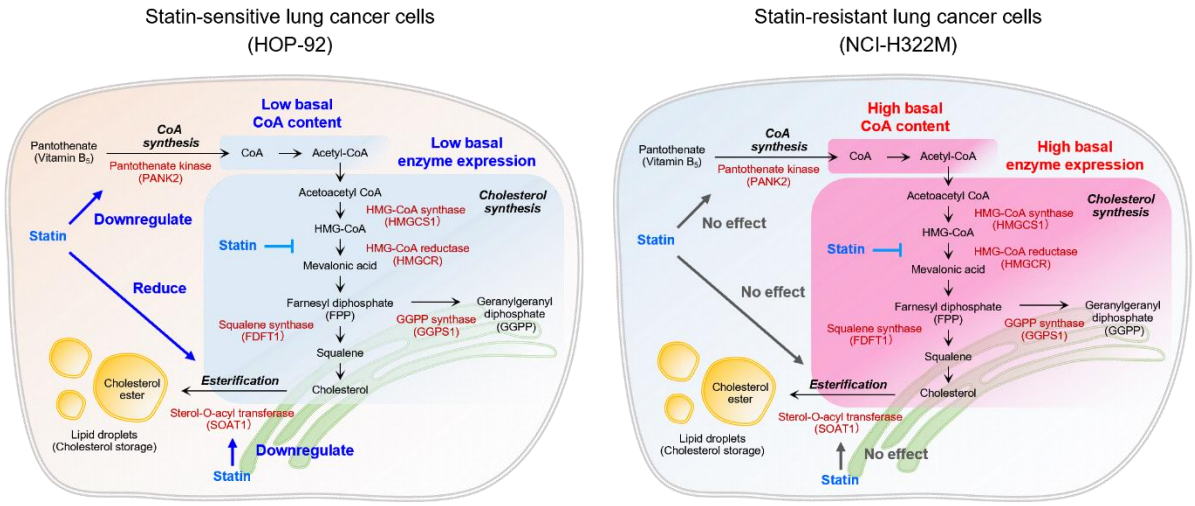

Fig. 8. Scheme of metabolic differences between statin-sensitive and statin-resistant lung cancer cells.

These schematic diagrams indicate dissimilarities in cholesterol-related metabolic processes between statin-sensitive HOP-92 cells and statin-resistant NCI-H322M cells. Statin-sensitive HOP-92 cells had lower CoA content and mevalonate pathway activity than statin-resistant NCI-H322M cells. CoA synthesis and cholesterol esterification may be affected by atorvastatin treatment through the downregulation of *PANK2* and *SOAT1* in HOP-92 cells. These findings suggest fundamental differences in cholesterol-related metabolism between statin-sensitive and statin-resistant cancer cells.